THE SPECTRUM OF THE RADIO BACKGROUND BETWEEN 13 AND 404 MHz

A. H. Bridle

Communicated by Dr J. E. Baldwin

Summary

Measurements of the brightness temperature of the radio background over a range of declinations at frequencies of $13 \cdot 15$, $17 \cdot 5$, and $81 \cdot 5$ MHz are described. Geometrically scaled aerials having beamwidths of $17° \times 12°$ and $53° \times 12°$ have been used, and the results are compared to deduce the spectrum of the background between these frequencies. The observed variation of the spectral index across the sky is fitted by a model in which the galactic contribution has temperature spectral indices $2 \cdot 38 \pm 0 \cdot 03$ and $2 \cdot 46 \pm 0 \cdot 04$ for two different regions of sky, superimposed upon an isotropic background due to radio galaxies, amounting to $30° \pm 7$ °K at 178 MHz. The galactic contributions are considered to be associated with radiation from the local spiral arm and from the inter-arm region, respectively.

The results are compared with those of other workers at $26 \cdot 3$, 38, $81 \cdot 5$, 178, and 404 MHz. In both regions, straight galactic spectra are found between $13 \cdot 15$ and 178 MHz, with temperature spectral indices $2 \cdot 38 \pm 0 \cdot 02$ and $2 \cdot 45 \pm 0 \cdot 03$. Both spectra steepen appreciably by 404 MHz, and it is concluded that the magnetic field strengths are very similar in the two regions. It is suggested that a change in the dominant production mechanism of cosmic ray electrons takes place at energies in the region of 3 GeV. The observed energy spectrum of primary cosmic ray electrons is shown to be consistent with that deduced from the new radio data.

1. *Introduction.* The spectrum of the large-scale structure of the cosmic radio background has been investigated by several workers in the northern hemisphere using geometrically scaled aerials (**1, 2, 3, 4**). Studies in the frequency range $26 \cdot 3$–404 MHz have shown that the spectrum of the total background varies across the sky (**2, 3**). This result has been interpreted as due to the superposition of a galactic component of constant spectral index whose intensity varies across the sky and an isotropic component having a different spectral index. Low-resolution studies extending the frequency range to $17 \cdot 5$, $13 \cdot 1$ and 10 MHz (**4**) have shown that there is no evidence for appreciable curvature of the galactic spectrum from 10 to 178 MHz.

The purpose of the work described in this paper has been to extend the investigation at the lower frequencies making use of greater resolving power, and so to test the conclusions drawn from the higher-frequency work.

2. *Experimental equipment.* Costain (**1**), Turtle *et al.* (**2**) and Purton (**3**) employed aerials of the $90°$ corner reflector type to provide a primary beam $44°$ in declination by $15°$ in right ascension. Direct extension of their work to lower frequencies was not feasible as geometrical scaling would necessitate unmanageably large aerial

14

structures. For observations at 13·15 and 17·5 MHz the transition was therefore made to a flat dipole array system whose beam could be swung in declination by adjusting the relative phases of the individual elements, and whose resolving power could be made as fine as required by filling a large enough area. New observations were also made at 81·5 MHz with such an array to provide comparison results at a higher frequency; in this way the spectra could be obtained independently of the temperatures measured by the earlier workers.

The aerial system employed at 17·5 and 81·5 MHz consisted of six parallel rows of four full-wave dipoles one wavelength apart aligned in the east–west direction. The rows were spaced 0·5 wavelengths apart in the north–south direction and were situated 0·125 wavelengths above a reflecting screen. The dipoles in each row were fed in phase and the relative phases of the rows were adjusted to swing the beam in declination. The feeding system allowed the use of the central pair of rows alone to provide a beam of width 53° in declination by 12° in right ascension between half power points. The half-power beamwidth of the whole array was 17° in declination by 12° in right ascension.

An aerial consisting of only two rows was constructed for use at 13·15 MHz, and results obtained with this have been compared with those obtained using only the central pair of rows in the 81·5 and 17·5 MHz arrays. The effects of mutual coupling between the dipoles in these arrays have been analysed by Pugh (5) and shown to have a negligible effect upon the amplitudes and phases of the currents excited in the central rows even when the beam is swung 30° from the zenith. Differences in beamshape between the 13·15 MHz rows standing alone and the central pairs of 81·5 and 17·5 MHz rows standing amidst the larger arrays are therefore thought to be negligible in this work. This is confirmed by observations made at 81·5 MHz in which these rows were used with their neighbours alternately open and short-circuited; it was found that the observed background temperatures were hardly affected by this procedure.

The receivers used at 13·15 and 17·5 MHz employed switching with synchronous detection in a similar way to those described by Andrew (4) and will not be discussed here. The receiver bandwidth is adjustable from 1·6 to 10 kHz. Rejection of high-level interfering signals at neighbouring frequencies is inadequate for radio astronomical purposes if the switching waveform contains appreciable harmonics outside this bandwidth. Earlier work at these frequencies using 300 Hz square-wave switching had been hindered by interference, and it was found that use of a 15 Hz square-wave switch appreciably improved the quality of the observations.

The 81·5 MHz receiver was similar to that at 178 MHz described in detail by Turtle *et al.* (2) and utilizes 180° switching with a hybrid ring circuit (6) to facilitate continual matching of the aerial to the receiver. The bandwidth was 1 MHz: the aerial was matched across the band using a high-level noise generator as a source of matching signal.

3. *Absolute calibration of the observations.* The temperature scale of the observations was established in terms of the noise output of a specially constructed 75 ohm coaxial diode noise generator whose output is expected to be constant to within 0·5% with frequency below 100 MHz (3). The gain of each receiver was measured daily by replacing the aerial with a matched diode noise generator calibrated in terms of the primary standard. This calibration can be made with relative accuracy

f $\pm 2\%$. Any error in the absolute scale of the primary standard will not introduce relative errors between the frequencies in this work, nor will it introduce a significant error in comparison with the earlier work at $26 \cdot 3$, 38, $81 \cdot 5$, 178 and 404 MHz 2, 3) as the temperature scales of these surveys have now been re-established by reference to the same standard (3).

Measurements were made of feeder losses on a number of occasions throughout the observations to detect possible long-term variations in feeder characteristics. Such measurements were found to repeat within the accuracy of measurement, which is $\pm 0 \cdot 1$ dB at all frequencies.

Imperfect reflexion by the ground screens was taken into account. At $13 \cdot 15$ and $17 \cdot 5$ MHz the screens consisted of parallel wires laid $0 \cdot 04$ wavelengths apart directly on the ground parallel to the dipoles in the arrays. The efficiency of such screens was verified in a subsidiary experiment described briefly in (4). A power loss of $0 \cdot 09$ dB was derived for both frequencies.

The screen used at $81 \cdot 5$ MHz was of similar construction, but was raised a few feet above the ground. The screen transparency has been calculated from an expression due to Mott (7), which gives good agreement with measurements of screen transmission in corner reflector aerials performed at the National Bureau of Standards (8). The power loss derived was $0 \cdot 15$ dB, or 3%. Aerial temperatures at this frequency were therefore corrected by subtracting the $9 \, ^\circ$K caused by thermal ground radiation and dividing by $0 \cdot 97$. The correction for ground radiation at the two lower frequencies is insignificant.

4. *The observations.* The basic observational programme consisted of taking drift curves with the $53^\circ \times 12^\circ$ beams at $13 \cdot 15$, $17 \cdot 5$ and $81 \cdot 5$ MHz centred in turn on declinations $+69^\circ$, $+52^\circ$, $+35^\circ$, and $+16^\circ$, and with the $17^\circ \times 12^\circ$ beams at $17 \cdot 5$ and $81 \cdot 5$ MHz centred on the same declinations. The sampling interval in declination is insufficient to permit the derivation of all the information obtainable with the narrower beam, but that has not been the aim of the present work, which is to provide directly comparable well-calibrated drift curves over a representative area of the northern sky.

Additional drift curves were taken at declinations $+40^\circ$, $+30^\circ$ and $+25^\circ$ with the $17^\circ \times 12^\circ$ beam at $81 \cdot 5$ MHz to determine the exact location of the region of minimum brightness temperature as seen with these aerials, and to provide information about the level of general background radiation against which the North Galactic Spur is seen. The Spur occupies most of the beamwidth to 3 dB points from right ascension 13^h to 18^h when the full resolution is used with the beam centre at declination $+16^\circ$. Drift curves were also taken with the $53^\circ \times 12^\circ$ beam centred on declinations $+60^\circ$ and $+40^\circ$, so that the temperature scale and zero level of the $81 \cdot 5$ MHz survey could be compared with Purton's observations at the same frequency (3), which have very similar resolution.

At $81 \cdot 5$ MHz observations were usually possible for twenty-four hours each day. The drift curves at a given declination repeated to $\pm 1\%$, except where the aerial became mismatched appreciably because of heavy rain or dew; such observations were discarded, as were those affected by appreciable interference, which originated mostly from electrical storms. All quoted brightness temperatures are the mean derived from at least two drift curves.

Observations at $13 \cdot 15$ and $17 \cdot 5$ MHz were possible only at night-time because of the high level of terrestrial interference at these frequencies during the day.

Very few records obtained in the period 1964 September–1965 May were completely free from interference, even though this period corresponded to minimum solar activity and should therefore have offered maximum protection from ionospherically-propagated transmissions. All brightness temperatures are derived from at least four observations obtained on nights when the region concerned was observed not less than 30 min before or after substantial interference, and the majority of temperatures have been derived from seven or eight such observations. The night-to-night repetition of records is not better than ±3%. Andrew (4) has shown that there is no correlation between background levels observed at night at these frequencies and corresponding values of f_0F_2. His analysis indicates that night-time ionospheric absorption is less than 2%. The poor repetition of records at the lower frequencies is attributed to the combined effects of low-level interference and absorption, and it has been assumed that the scatter is randomly distributed. Particular emphasis was placed upon the observations of the region of minimum brightness temperature which was shown by the 81·5 MHz survey to lie at right ascension 09^h 30^m, declination +35°, and all the observations used in the reduction of this region were made in the four hours before sunrise when observing conditions were consistently better than average. This region was observed at 17·5 MHz with the full resolution every night for ten successive nights on which it was free from interference, and the temperatures here are thought to be as reliable as those at 81·5 MHz (±1%).

The derived sky brightness temperatures are given in Tables I–III.

The errors to which the observations are liable may be summarized as follows: (i) errors in the absolute scale of noise source calibrations, being ±4% at all frequencies, (ii) combined errors in the measurement of feeder losses, etc., being ±2% at all frequencies, and (iii) the night-by-night scatter of the drift curves as described above. The first two sources of error do not affect the relative accuracy of temperatures for different regions of sky at the same frequency and hence do not affect the detection of variations in spectral index, which is limited purely by inexact repetition of the records. We may thus investigate differences in spectral index from one part of the sky to another within finer limits than we may determine the value of the index absolutely at any one point.

Table IV presents the estimated errors in various quantities which may be derived from the observations.

5. *Spectral analysis of results*

(a) *Total background spectral index.* The only parameter of the background radiation which can be derived without ambiguity from the three surveys is the spectrum of the total background radiation. A point-by-point comparison of any pair of surveys with the same beam at frequencies v_1 and v_2 enables a map of β defined by $(T_1/T_2)=(v_2/v_1)^\beta$ to be derived. Fig. 1 shows the map of β obtained by comparing the 17°×12° results at 17·5 and 81·5 MHz. The maps derived from the three lower-resolution surveys show essentially the same features. The contour interval is 0·025 in β, i.e. a factor of 1·05 in temperature ratio, and therefore taken at the estimated significance level of variations in β. Fig. 2 shows the contours of constant sky brightness temperature with this resolution at 17 MHz, with a contour interval of 10 000 °K.

Comparison of the brightness temperature map with that of β shows that the contours are fairly well aligned over much of the northern sky covered in the

TABLE I

Sky brightness temperatures at 13·15 MHz with beam 53° × 12°. The unit is 1 000 °K

h m	$\delta = 69°$	$\delta = 52°$	$\delta = 35°$	$\delta = 16°$
00 00			148	
00 30			144	
01 00			144.	
01 30			150	
02 00		146	148	
02 30		147	147	
03 00	171	148	146	
03 30	171	148	146	
04 00	169	151	149	
04 30	165	152	153	
05 00	160	152	156	
05 30	155	150	152	
06 00	148	140	145	
06 30	136	131	138	
07 00	128	121	129	
07 30	122	113	117	
08 00	114	103	106	
08 30	104	94	93	
09 00	100	89	84	
09 30	98	87	82	
10 00	98	87	81	
10 30	99	89	87	
11 00	101	92	91	101
11 30	104	96	95	104
12 00	107	99	98	109
12 30	109	101	104	112
13 00	112	104	107	116
13 30	114	108	112	119
14 00	117	112	117	123
14 30	118	117	123	127
15 00	122	121	135	132
15 30	125	127	145	140
16 00	127	131	151	148
16 30	131	139	159	156
17 00	135	147	167	170
17 30	141	160	180	183
18 00	150	174		202
18 30	158	185		
19 00		192		
19 30				
20 00				
20 30				
21 00				
21 30				
22 00			171	
22 30			166	
23 00			159	
23 30			153	

148

TABLE II

Sky brightness temperatures at 17·5 MHz. The unit is 100 °K

h	m	(a) Beam 12°×17° δ=69°	δ=52°	δ=35°	δ=16°	(b) Beam 12°×53° δ=69°	δ=60°	δ=52°	δ=35°	δ=16°
00	00			655						
00	30			·640				800	705	
01	00	895	790	610			840	770	705	
01	30	895	785	640		865	835	765	705	
02	00	890	790	660		870	850	775	710	
02	30	880	825	670		860	860	785	725	
03	00	860	850	705		850	855	790	720	
03	30	845	885	690		840	850	790	710	
04	00	835	890	720	695	835	840	795	720	610
04	30	825	875	750	760	830	835	805	735	665
05	00	765	840	785	845	795	820	790	770	710
05	30	740	795	800	900	785	790	790	770	730
06	00	710	735	760	945	740	735	735	745	745
06	30	680	690	705	835	705	690	675	710	715
07	00	650	640	655	705	665	650	625	665	675
07	30	615	595	600	610	630	600	585	610	615
08	00	595	535	520	535	585	545	540	545	550
08	30	575	485	450	470	545	505	505	480	485
09	00	565	445	390	420	520	475	465	425	440
09	30	560	415	355	420	510	450	435	410	435
10	00	545	400	380	440	530	460	440	425	445
10	30	560	410	415	470	535	480	460	455	470
11	00	565	425	450	490	550	490	475	485	500
11	30	580	440	490	530	565	500	500	505	535
12	00	580	460	510	565	580	525	530	540	570
12	30	580	475	525	640	585	535	540	560	600
13	00	580	480	545	675	595	550	555	590	610
13	30	590	490	565	710	605	555	565	615	630
14	00	605	500	600	765	610	580	595	640	665
14	30	625	525	640	835	625	600		680	715
15	00	650	540	675	910	640	630		725	765
15	30	670	565	710	980	640			770	790
16	00	705	595	740	1050	645			805	825
16	30	720	625	740	1140	650			845	870
17	00	740	670	765	1220	660			890	945
17	30	750	715	835	1310	675			945	1020
18	00	765	780	905	1420	690			1055	1115
18	30	775	845	1000	1505	725				1225
19	00	785	905		1615	760				1280
19	30	785	1020		1540	795				1230
20	00	785			1160	820				1140
20	30				890					1010
21	00		915	805	790					910
21	30		890	780						
22	00			760						
22	30			720						
23	00			685						
23	30			670						

TABLE IIIa

Sky brightness temperatures at 81·5 MHz with beam 12° × 17°. The unit is 1 °K

h m	$\delta=69°$	$\delta=52°$	$\delta=40°$	$\delta=35°$	$\delta=30°$	$\delta=25°$	$\delta=16°$
00 00		2240		1505			1440
00 30		2140		1425			1440
01 00	2270	2045		1415			1440
01 30	2160	2005		1425			1440
02 00	2205	1980		1480			1580
02 30	2160	2010		1545			1640
03 00	2095	2055		1565			1640
03 30	1985	2100		1580			1540
04 00	1880	2125		1620			1575
04 30	1780	2105		1745			1715
05 00	1695	2045		1900			1910
05 30	1665	1875		1850			2045
06 00	1590	1690		1725			2125
06 30	1540	1545		1580			1920
07 00	1450	1420		1435			1570
07 30	1395	1295		1280			1310
08 00	1315	1135		1120			1160
08 30	1280	1030		980			980
09 00	1220	950	820	800	820		885
09 30	1205	865	760	680	780		885
10 00	1195	855	740	775	820		915
10 30	1215	855	755	840	835		960
11 00	1215	890	790	880	885		1000
11 30	1225	910	845	935			1050
12 00	1230	940		1000			1120
12 30	1235	950		1020			1230
13 00	1235	950		1030			1330
13 30	1245	980		1100			1430
14 00	1285	990	1115	1145	1225	1515	1610
14 30	1305	1030	1185	1235	1320	1715	1825
15 00	1345	1070	1270	1310	1390	1850	2020
15 30	1360	1120	1300	1370	1455	1940	2195
16 00	1420	1160	1370	1435	1545	2055	2400
16 30	1490	1225	1465	1510	1615	2180	2560
17 00	1530	1290	1690	1585	1660	2230	2690
17 30	1630	1420	1635	1695	1705	2300	2870
18 00	1715	1635	1850	1940	1915	2555	3175
18 30	1750	1885	2190	2220			3390
19 00	1770	2045		2565			3630
19 30	1775	2280		3380			
20 00	1785			4000			3315
20 30				3825			2625
21 00	1815	2945		2855			2205
21 30		2785		2490			1965
22 00	2025	2690		2115			1780
22 30		2655		1855			1655
23 00	2350	3150		1600			1505
23 30		3295		1545			1455

TABLE IIIb

Sky brightness temperatures at 81·5 MHz with beam 12° × 53°. The unit is 1 °K

h	m	$\delta=69°$	$\delta=60°$	$\delta=52°$	$\delta=40°$	$\delta=35°$	$\delta=16°$
00	00	2430	2250	1935	1815	1740	1345
00	30	2220	2040	1825	1675	1625	1295
01	00	2115	1950	1800	1665	1610	1265
01	30	2115	1940	1800	1665	1615	1310
02	00	2140	1970	1840	1695	1655	1345
02	30	2115	1975	1910	1705	1655	1390
03	00	2115	1970	1910	1735	1655	1395
03	30	2140	1950	1885	1735	1670	1405
04	00	2030	1955	1840	1745	1700	1440
04	30	1975	1885	1840	1755	1735	1505
05	00	1910	1845	1860	1770	1745	1585
05	30	1800	1770	1840	1765	1760	1650
06	00	1695	1675	1680	1725	1735	1670
06	30	1590	1545	1505	1605	1590	1640
07	00	1490	1415	1370	1430	1500	1495
07	30	1380	1305	1275	1220	1320	1330
08	00	1285	1200	1155	1085	1140	1170
08	30	1185	1115	1060	950	995	995
09	00	1140	1060	985	885	885	945
09	30	1090	1045	925	855	820	925
10	00	1065	1025	925	855	835	950
10	30	1085	1025	950	885	865	985
11	00	1115	1040	970	925	910	1070
11	30	1130	1070	1000	940	965	1110
12	00	1130	1115	1045	975	1020	1140
12	30	1130	1160	1080	1020	1050	1220
13	00	1130	1185	1090	1060	1115	1275
13	30	1175	1200	1120	1125	1175	1310
14	00	1195	1240	1170	1185	1250	1360
14	30	1215	1275	1225	1290	1335	1445
15	00	1240	1310	1290		1440	1545
15	30	1260	1345	1350		1535	1630
16	00	1285		1415		1630	1740
16	30	1330		1485		1725	1860
17	00	1380		1535		1915	2045
17	30	1455		1600		2250	2335
18	00	1590		1750		2600	2825
18	30	1680		1905			3330
19	00	1800		2430			3590
19	30	1950					3330
20	00	2240					2875
20	30						2440
21	00						1940
21	30						
22	00					1975	
22	30					1885	
23	00					1845	
23	30					1805	
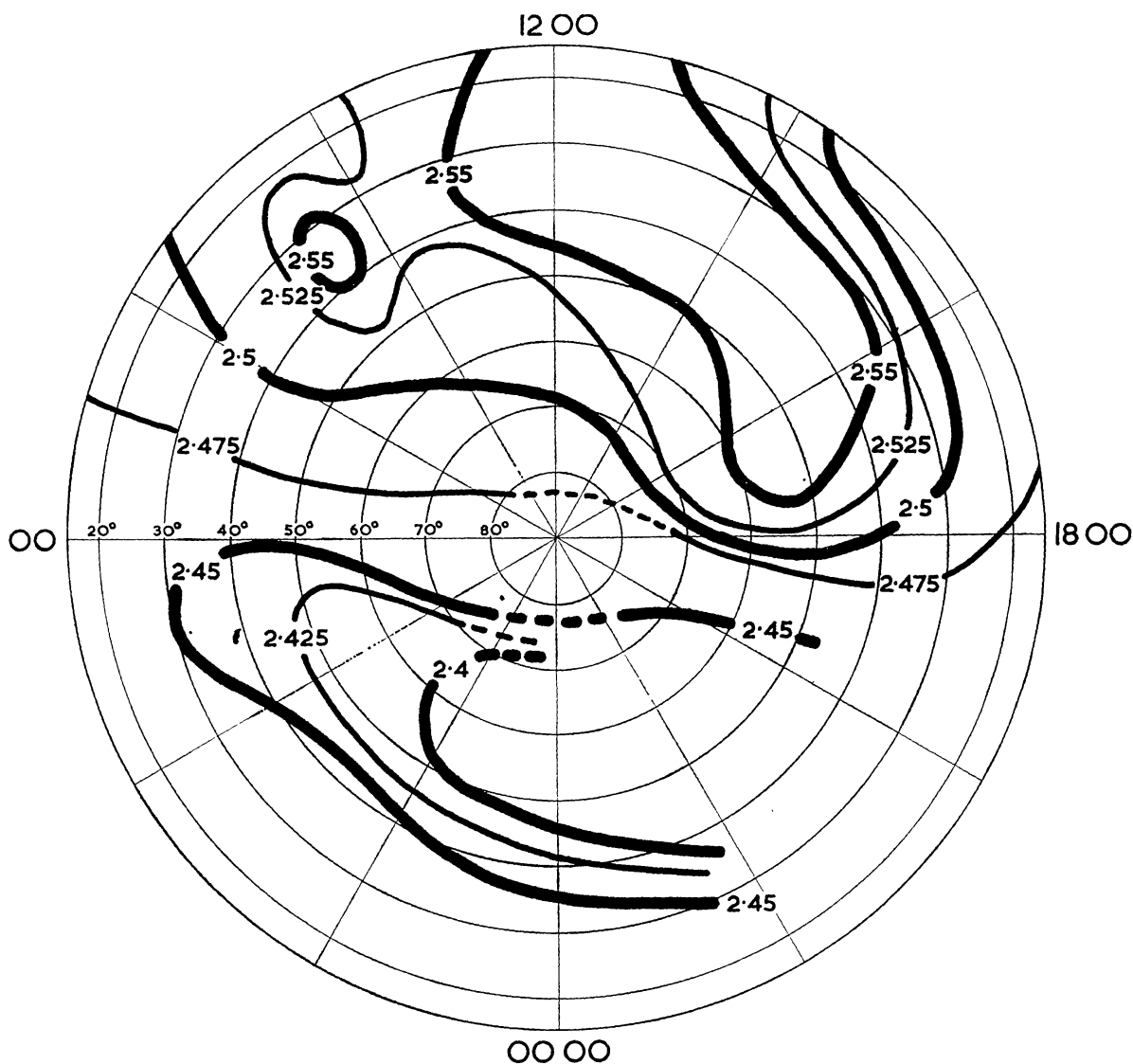
FIG. 1. *Contour map of β between 17·5 and 81·5 MHz, beamwidth 17°×12°.*

TABLE IV

Estimated errors in the observations

ν (MHz)	R.m.s. calibration error (%)	R.m.s. repetition error (%)	R.m.s. absolute level error (%)	Maximum absolute level error (%)
81·5	4	1	3	7
17·5	4	3	5	9
13·15	4	3	5	9

$\Delta\nu$ (MHz)	R.m.s. error in β at any point	Max error in β	Significance level of variation in β
81·5–17·5	±0·04	±0·09	±0·025
81·5–13·15	±0·04	±0·08	±0·025

work, and that β is generally high in regions of low brightness temperature and vice versa. These results are consistent with the interpretation that the total background is compounded of a contribution with a moderately flat spectrum,
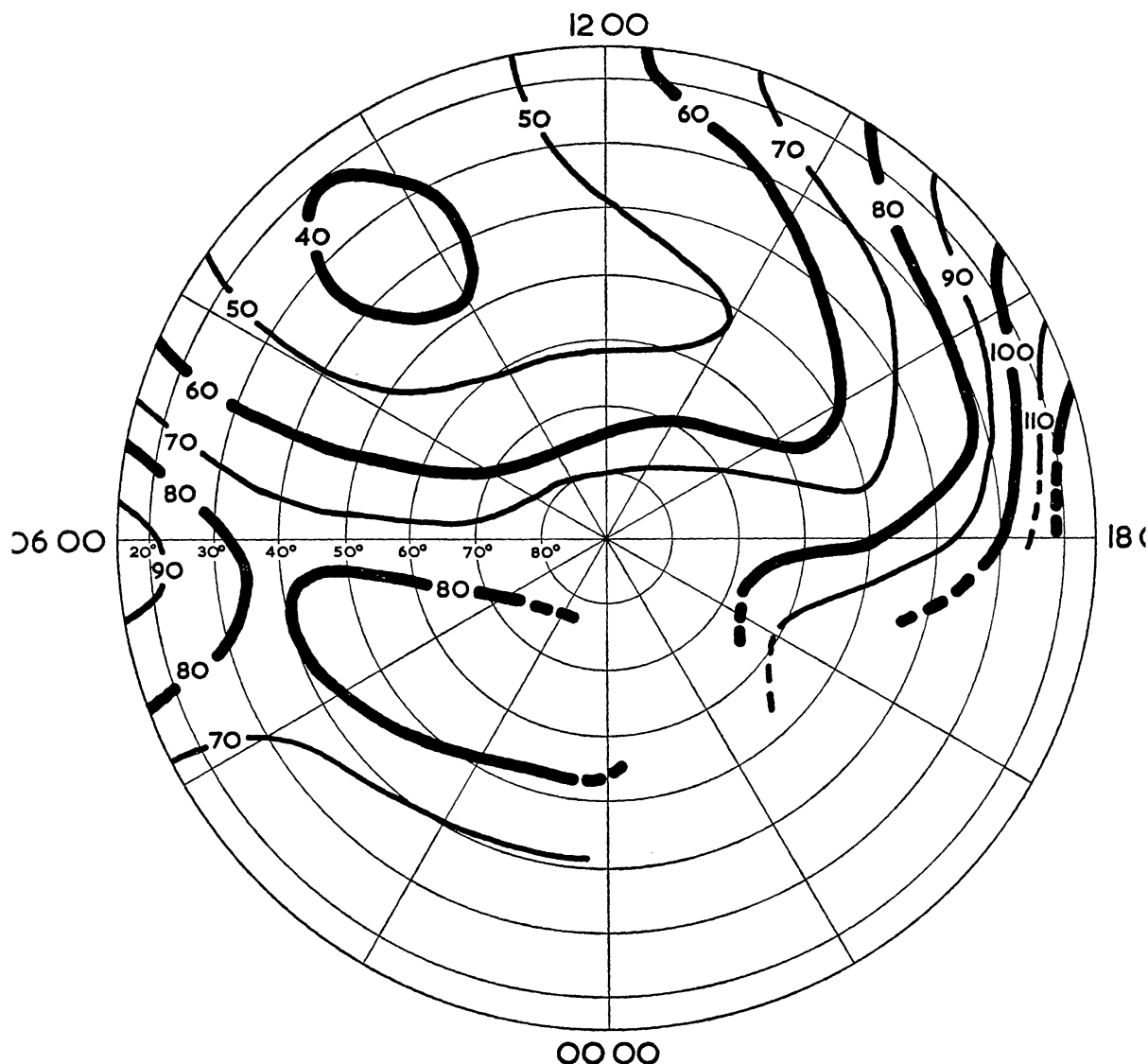
FIG. 2. *Contour map of sky brightness at* 17·5 *MHz, beamwidth* 17 ° × 12 °.

whose brightness varies across the sky, and an isotropic contribution with a steep spectrum. The total spectral index would take high values in regions where the anisotropic component contributed little radiation, and in which therefore the total sky brightness is small. The contours of β and those of temperature at any one frequency would be perfectly aligned if the anisotropic component had the same spectral index everywhere. Such a simple model cannot account for all the details of the observed variation of total spectral index across the sky. For example, there is no feature in the brightness contours which corresponds to the region of high spectral index around the North Galactic Pole and elongated towards right ascension 17ʰ, declination + 50°. This failure of the simple model will now be considered further in detail.

(b) *The differential spectrum.* It has been noted (1, 2, 3) that if the background radiation consists of isotropic radiation with spectral index β_0, and superimposed anisotropic radiation with constant spectral index β_1, a plot of temperatures at one frequency against temperatures observed at the same beam positions at another

will yield a straight line whose slope is determined by β_1. This plot will be called
a T–T plot in what follows and the spectrum defined by β_1 will be called the
differential spectrum. The general appearance of a T–T plot of the new measure-
ments at a given declinaton is shown in Fig. 3, which was obtained using the
$17° \times 12°$ drift curves on declination $+52°$ at $17\cdot5$ and $81\cdot5$ MHz. It is evident
that on such a model the index β_1 must itself vary across the sky, as significant
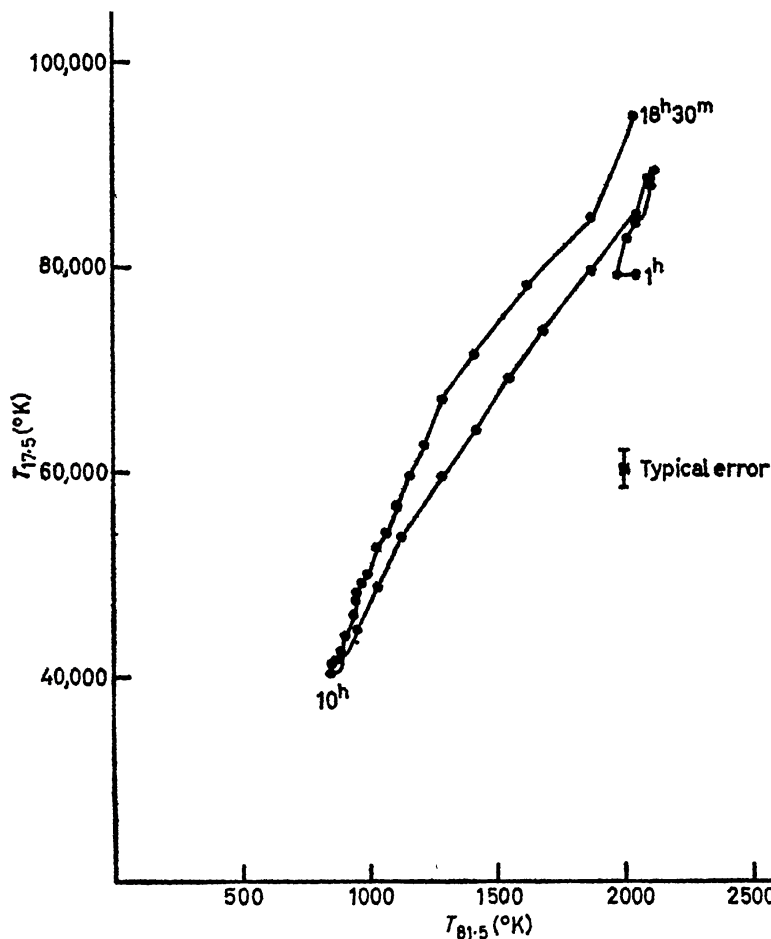
FIG. 3. T–T plot of new measurements, $17\cdot5$ and $81\cdot5$ MHz, beamwidth $17° \times 12°$,
$\delta = +52°$.

departures from linearity of the plot occur over a wide range of aerial beam posi-
tions. This effect occurs in all the surveys of the present work, and is not thought
to be of instrumental origin. It cannot have arisen from the necessity to observe
different regions of sky at different times of year at the low frequencies, for the
observations were arranged so that as many hours of right ascension as possible
were overlapped on successive sets of drift curves at the same declination; this
would have enables seasonal effects, e.g. effects arising from long-term variations
in ionospheric parameters, to be detected. The effect may also be seen in the
higher-frequency results of (3), where it is, however, of the same order as the
anticipated errors in the observations.

It is likely that observations close to the galactic equator will be affected at the
lower frequencies by absorption of the radiation in ionized hydrogen regions.
The extent of this effect is hard to anticipate as there is no high-resolution study
of the appropriate area of sky available at these frequencies. Observations made

in the southern hemisphere (9) indicate that strongly absorbing regions are confined to galactic latitudes less than 10° at 13 MHz. In the first analysis, positions of the aerial beam for which the centre lies at galactic latitudes less than 15° were omitted.

Turtle *et al.* (2) and Purton (3) derive differential spectra for two areas of sky defined by (1) $\alpha = 03^h–10^h$, (2) $\alpha = 10^h–17^h$, all declinations. These definitions separated high and low galactic latitudes adequately for their purpose, but the present work, using higher resolution and lower frequencies, shows that the differential spectrum is not constant within these regions. The new results have been analysed over two regions defined by their relation to the spiral structure of the Galaxy as indicated by 21-cm observations (10) as follows:

Region 1 $l^{II} = 140°$ to 220°   Region 2 $b^{II} > 70°$, all l^{II}

  $15° < b^{II} \leqslant 50°$ $70° \geqslant b^{II} > 50°$ $l^{II} = 50°$ to 90°

                                              $50° \geqslant b^{II} \geqslant 30°$ $l^{II} = 70°$ to 90°

The division of the sky into regions for analysis must include in each region a sufficiently large temperature variation for the differential spectrum to be derivable with accuracy; in each of the regions taken here, there is a 2 : 1 variation of observed brightness temperatures at 81·5 MHz using the full resolving power. In Region 1 most of the galactic radiation, even at these latitudes, is expected to be non-thermal emission from electrons moving in the magnetic field of the nearby spiral arm (11). In Region 2, the radiation is from directions in the interarm region, leaving out the direction of the North Galactic Spur.

Both regions exhibit linear $T–T$ plots, and are therefore characterized by constant differential spectra; the parameters of these spectra are given in Tables V and VI, and were determined by fitting lines to the data using a least-squares

TABLE V

Differential spectrum of Region 1

ν (MHz)	$T/T_{81·5}$	$S/S_{81·5}$	Spectral index β_1
17·5	39 ± 2	1·79 ± 0·11	2·38 ± 0·03
13·15	76 ± 5	1·98 ± 0·12	2·38 ± 0·04

TABLE VI

Differential spectrum of Region 2

ν (MHz)	$T/T_{81·5}$	$S/S_{81·5}$	Spectral index β_1
17·5	45 ± 2·5	2·04 ± 0·12	2·475 ± 0·04
13·15	87 ± 5	2·27 ± 0·13	2·45 ± 0·04

procedure which took into account the greater accuracy of repetition of the 81·5 MHz result. The $T–T$ plots and the fitted lines are shown in Figs. 4 and 5. The two differential spectra are not the same within their r.m.s. errors. The probability of these results being obtained from two regions which in fact have the same differential spectra is 1 in 15.

The difference between the derived differential spectra in the two regions suggests that the measurements at low galactic latitudes in Region 1 could be
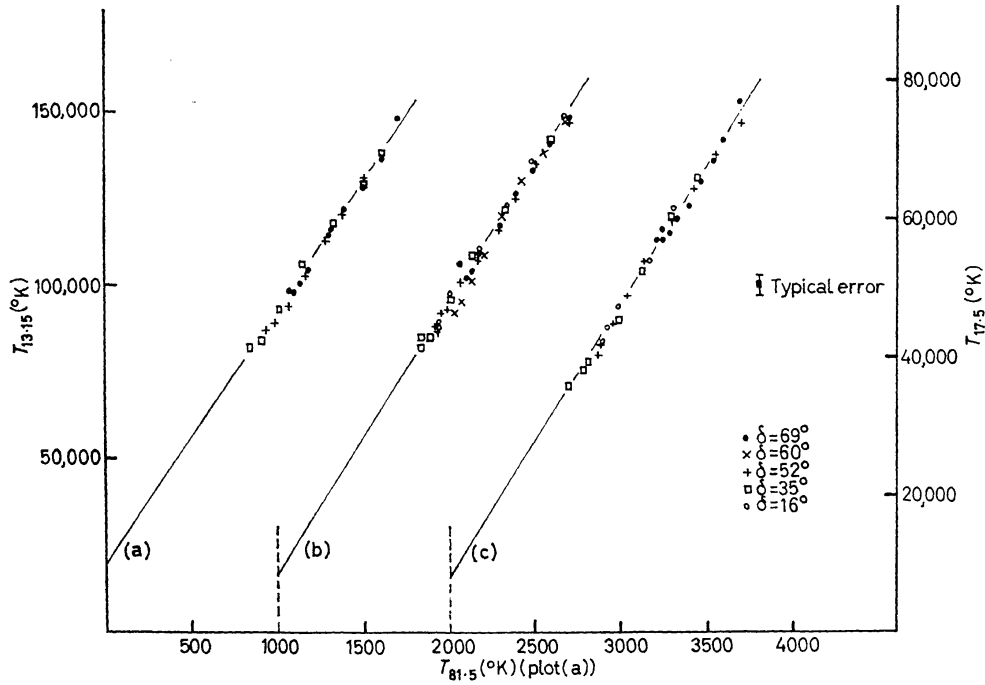
FIG. 4. *T–T* plots in Region 1.
(a) 13·15 and 81·5 MHz, beamwidth 53° × 12°.
(b) 17·5 and 81·5 MHz, beamwidth 53° × 12°.
(c) 17·5 and 81·5 MHz, beamwidth 17° × 12°.
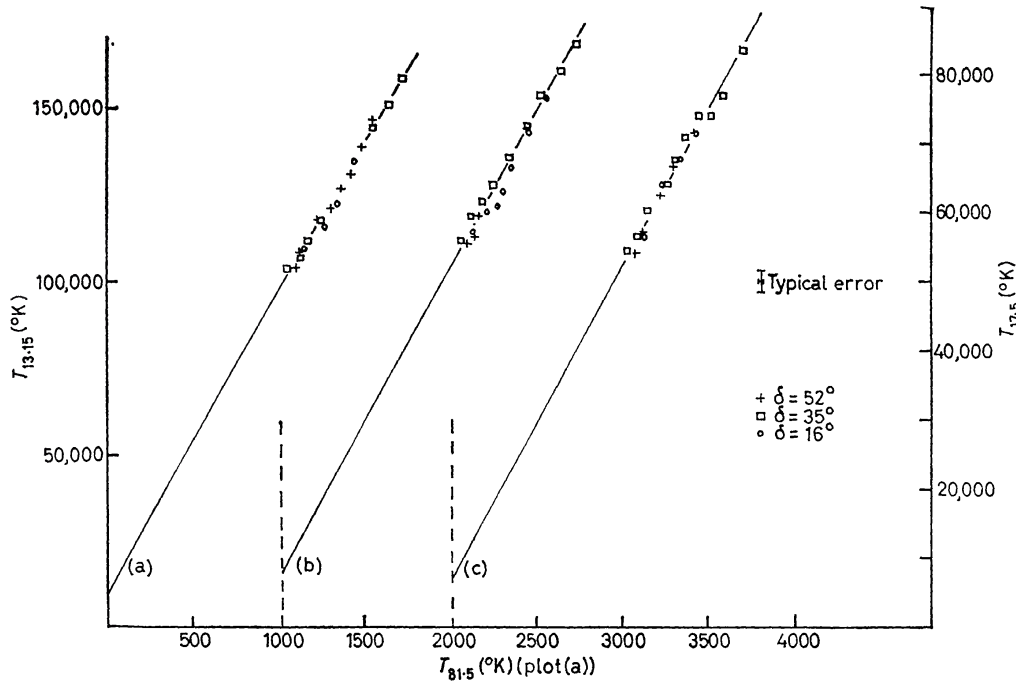
FIG. 5. *T–T* plots in Region 2.
(a) 13·15 and 81·5 MHz, beamwidth 53° × 12°.
(b) 17·5 and 81·5 MHz, beamwidth 53° × 12°.
(c) 17·5 and 81·5 MHz, beamwidth 17° × 12°.

TABLE VII

Differential spectrum of restricted Region 1

	$T_{17\cdot5}/T_{81\cdot5}$	$T_{13\cdot15}/T_{81\cdot5}$
(a)	$38\cdot5\pm2$	76 ± 5
(b)	40 ± 3	73 ± 7

affected by HII absorption despite the exclusion of the strip about the galactic equator. This was tested by re-analysing the data in this region omitting beam positions centred on latitudes less than (a) $20°$ and (b) $30°$. The results of this analysis are shown in Table VII. The differences produced by reducing the range of galactic latitudes in Region 1 are seen to be insignificant. Studies of the galactic plane with higher resolution at these frequencies would be needed to establish firmly that the effects of absorption in the disc in this work are negligible, but we shall draw the tentative conclusion that this is the case.
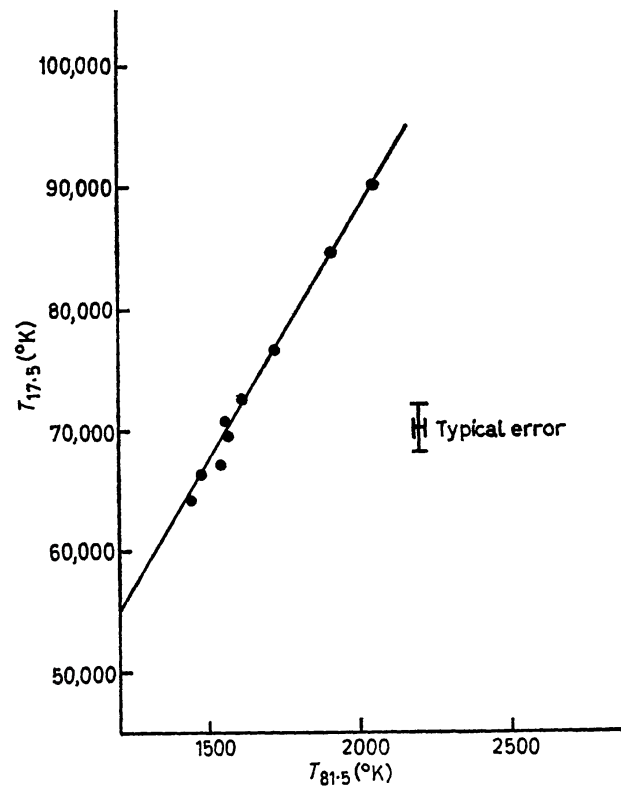
FIG. 6. *T–T plot at negative galactic latitudes, $17\cdot5$ and $81\cdot5$ MHz, beamwidth $17° \times 12°$.*

Many points on the T–T plots corresponding to positions of the beam centre in the range $-15° \leqslant b^{\mathrm{II}} \leqslant +15°$ lie significantly below the line fitted to Region 1. HII absorption can therefore be detected along the galactic equator at these frequencies, in agreement with the results of southern workers.

Fig. 6 shows a T–T plot for the region corresponding to Region 1 at negative galactic latitudes with the best-fitting line for positive latitudes superposed. Because the data do not extend below $b^{\mathrm{II}} = -30°$ one cannot be sure that the whole of this region has the same differential spectrum as Region 1, but the available evidence suggests that this is so.

Points on the T–T plots corresponding to directions in the region of the North

Galactic Spur lie significantly below the line fitted to Region 2, of which the Spur orms a boundary. If the galactic background against which the Spur is seen has he differential spectrum of Region 2, which is probable because of its position n the inter-arm region, this would imply that the Spur radiation has a lower spectral index than most of its surroundings. Using the estimate of the brightness of the isotropic component derived in the next section, we find that the spectrum of the Spur between $17 \cdot 5$ and $81 \cdot 5$ MHz must have a β of $2 \cdot 1 \pm 0 \cdot 2$ between right ascensions 14^h and 16^h 30^m.

6. *The isotropic component.* The radiation from all discrete extragalactic radio sources which could be detected individually down to a flux density of $0 \cdot 25 \times 10^{-26}$ w.m^{-2} Hz^{-1} at 178 MHz, the limit of the survey by Ryle & Neville (12), contributes a brightness temperature averaged over the sky of $\sim 10\,^{\circ}$K at this frequency. The magnitude of this contribution leads us to examine a model in which the postulated isotropic component consists entirely of the integrated emission from such sources.

There is little published data on the spectra of extragalactic sources at frequencies below 20 MHz. The spectra of a considerable number have been determined down to 38 MHz (13) and $26 \cdot 3$ MHz (14) however, and there is good evidence that about 80% of the sources have straight spectra from about 1500 MHz to these frequencies. Preliminary results of observations by the author of over 100 radio sources using the $10 \cdot 03$ MHz array at the Dominion Radio Astrophysical Observatory (15, 16) indicate (a) that there is no appreciable downward curvature in the spectra of the majority of sources away from the galactic equator at this frequency, and (b) that the mean spectral index for extragalactic sources in the frequency range of the present work is $\beta_0 \approx 2 \cdot 75$, with a probable error of $\pm 0 \cdot 2$.

It is well-known that some sources of high surface brightness temperature exhibit downward spectral curvature below 50 MHz. Many of these sources are also of high intrinsic power. The spatial density of such sources is likely to be low, and their contribution to the integrated emission will be much smaller than that of individually less powerful sources of much higher spatial density.

The normal galaxies, whose radio luminosities are $< 10^{23}$ w. Hz^{-1} ster^{-1} at 178 MHz, form a class of this second type. The importance of their contribution to the integrated emission depends on the cosmological model assumed for them. Assuming the luminosity distribution of this class of source derived by Longair & Scott (17), it may be shown that the integrated emission expected from them at 178 MHz is $\leqslant 3\,^{\circ}$K on either the steady-state or the Einstein–de Sitter cosmology. It is however well known that the number counts of radio sources at different flux densities are inconsistent with simple cosmological models. Gower (18) has derived a model for the source counts in which the spatial density of radio sources varies with the cosmological epoch. The integrated emission calculated for the normal galaxies at 178 MHz on the basis of the same density variation exceeds the minimum sky brightness temperature of $65 \pm 5\,^{\circ}$K observed by Turtle & Baldwin (19) by a factor of three. It follows that the normal galaxies cannot exhibit such a density variation. An analysis of the source counts by Longair (20) in terms of the evolution of the luminosities of radio sources with cosmological epoch has led to a similar conclusion. We shall therefore assume that the integrated emission from the normal galaxies is of the order expected from the steady-state or the Einstein–de Sitter models and will neglect it in what follows.

It follows from the above discussion that the dominant contribution to the integrated emission will be that of radio galaxies whose luminosities lie in the range 10^{23} to 10^{26} w.Hz^{-1} ster^{-1} at 178 MHz.

Table VIII summarizes the parameters of the isotropic component which will fit the present observations as a function of the assumed value of β_0 together with

TABLE VIII

Fitted parameters of isotropic component

Assumed β_0	$T_{13 \cdot 15}$	$T_{17 \cdot 5}$	$T_{81 \cdot 5}$	T_{178}	T_{178} (Turtle)
2·6	$53 \pm 11 \cdot 10^3$	$23 \pm 5 \cdot 10^3$	480 ± 100	46–69	40–80
2·7	$41 \pm 10 \cdot 10^3$	$19 \pm 4 \cdot 10^3$	300 ± 60	29–45	30–55
2·8	$33 \pm 7 \cdot 10^3$	$14 \pm 3 \cdot 10^3$	200 ± 40	18–28	20–35
2·9	$25 \pm 5 \cdot 10^3$	$12 \pm 3 \cdot 10^3$	140 ± 30	12–18	14–27

the values derived by Turtle *et al.* The new estimations, made by combining the assumed value of β_0 with the line fitted to Region 2, agree with the earlier results, but the error for a given β_0 here is smaller because of the greater importance of the steep spectrum at the lower frequencies of this work. It may be seen that the uncertainty in the magnitude of the isotropic component arising from the uncertainty in the best value of β_0 is greater than that arising from the errors in the present observations. For the best estimate of $\beta_0 = 2 \cdot 75$ given above, the brightness of the extragalactic integrated emission at 178 MHz, T_{178}, is $30 \pm 7\,^\circ$K. This is equivalent to $14\,000 \pm 3\,000\,^\circ$K at 19·7 MHz, which is in agreement with Shain's estimate of $7\,000^\circ$–$22\,000\,^\circ$K at this frequency based on observations of 30 Doradus (**21**).

7. *Comparison with results of other workers*

(a) *Temperature scales.* Comparison of Table IIIb with the corner-aerial results of Purton (**3**), where common declinations are available, enables the compatibility of the two 81·5 MHz temperature scales and zero levels to be verified. After
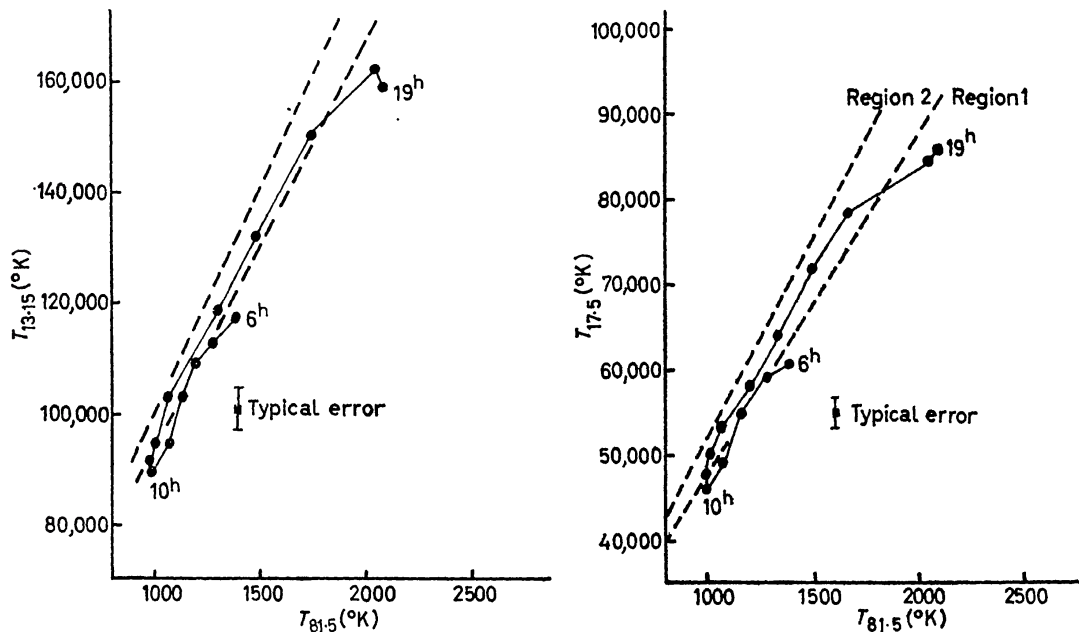

FIG. 7. *T–T plots of single-dipole measurements, 13·15 and 17·5 MHz against 81·5 MHz.*

allowance for the differing resolutions of the two aerial systems, the temperatures are in good agreement within the quoted errors. Comparison has also been made with the single-dipole results of Andrew (4) at $13 \cdot 1$ and $17 \cdot 5$ MHz by making observations at $81 \cdot 5$ MHz with a dipole scaled to his design. Fig. 7 shows the T–T plots between the three frequencies $13 \cdot 1$, $17 \cdot 5$, and $81 \cdot 5$ MHz obtained with these aerials, which are in good agreement with the lines fitted to Regions 1 and 2 (also shown), bearing in mind that Region 2 never fills the beam of a single dipole.

(b) *Differential spectra.* Lines have been fitted to T–T plots of the sky brightness temperatures of Turtle *et al.* and Purton, using Purton's calibrations, in the regions of sky selected in the present work. For each pair of frequencies the slope of the line in each region defines a temperature ratio T_1/T_2. These ratios have been converted into flux density ratios by the relation

$$T_1/T_2 = (\nu_2/\nu_1)^2 \, S_1/S_2,$$

and the results combined to derive the differential flux density spectra shown in Figs. 8a and 8b. These spectra are normalized to unit flux density at $81 \cdot 5$ MHz and include the points derived from the new results. Both spectra are straight within the limits of error between 178 and $13 \cdot 15$ MHz, but the positions of the 404 MHz points require steepening of both spectra to a flux spectral index $\alpha \approx 0 \cdot 9$ ($\beta \approx 2 \cdot 9$) above $\nu \approx 200$ MHz. Slight curvature over the whole frequency range is possible within the error limits for Region 1, the tangential spectrum then becoming as steep as the spectrum of Region 2 by $\nu \approx 100$ MHz; the spectra of the two regions cannot be superimposed simply by changing the frequency scale of one of them, as would be possible if they arose from the same distribution of energies of the radiating electrons but with different magnetic fields in the emitting regions. This is a result of the relatively low values of the 404 MHz points, and new observations are being made at 610 MHz to check this implied steepening of the spectra at high frequencies. Such steepening, occurring at the same frequency in both spectra, would imply that the arm and inter-arm regions have similar magnetic field strengths and electron energy spectra which steepen remarkably by about unity in the index γ appearing in $N(E) = kE^{-\gamma}$ for energies of a few GeV.

(c) *Correlation with cosmic-ray experiments.* Wentzel (21) has used the flux of primary cosmic-ray electrons at the top of the Earth's atmosphere measured by Earl (22) to derive a mean magnetic field in the local spiral arm of $H \approx 2 \times 10^{-5}$ gauss by considering the observed brightness of synchrotron radio emission. Parker (24) has investigated the effect of exclusion of galactic electrons from the solar system by the solar wind, and it seems that Earl's measured flux may be as much as an order of magnitude below the true galactic flux. In this case a value of $0 \cdot 5$–$1 \cdot 10^{-5}$ gauss would be a better estimate for the field strength. This is still higher than the field compatible with the attempts to observe Zeeman splitting of the 21 cm line of neutral hydrogen by Morris *et al.* (25) and Weinreb (26). For the purpose of comparing the observed radio synchrotron emission spectrum with the measured energy spectrum of cosmic-ray electrons we shall tentatively assume a mean field of 5×10^{-6} gauss in our Region 1. In such a field the frequency range 13–404 MHz corresponds to electron energies of 750 MeV–4 GeV, where we assume that a single electron radiates only at the frequency $\nu_{\max}$ corresponding to the peak of its actual power radiation spectrum $P(\nu)$. The observed differential

radio spectrum of Region 1 implies an electron energy spectrum with

$$\gamma = 1 \cdot 76 \pm 0 \cdot 04$$

from 750 MeV to 2·8 GeV, steepening to $\gamma \approx 2 \cdot 8$ near 3 GeV. We have used here
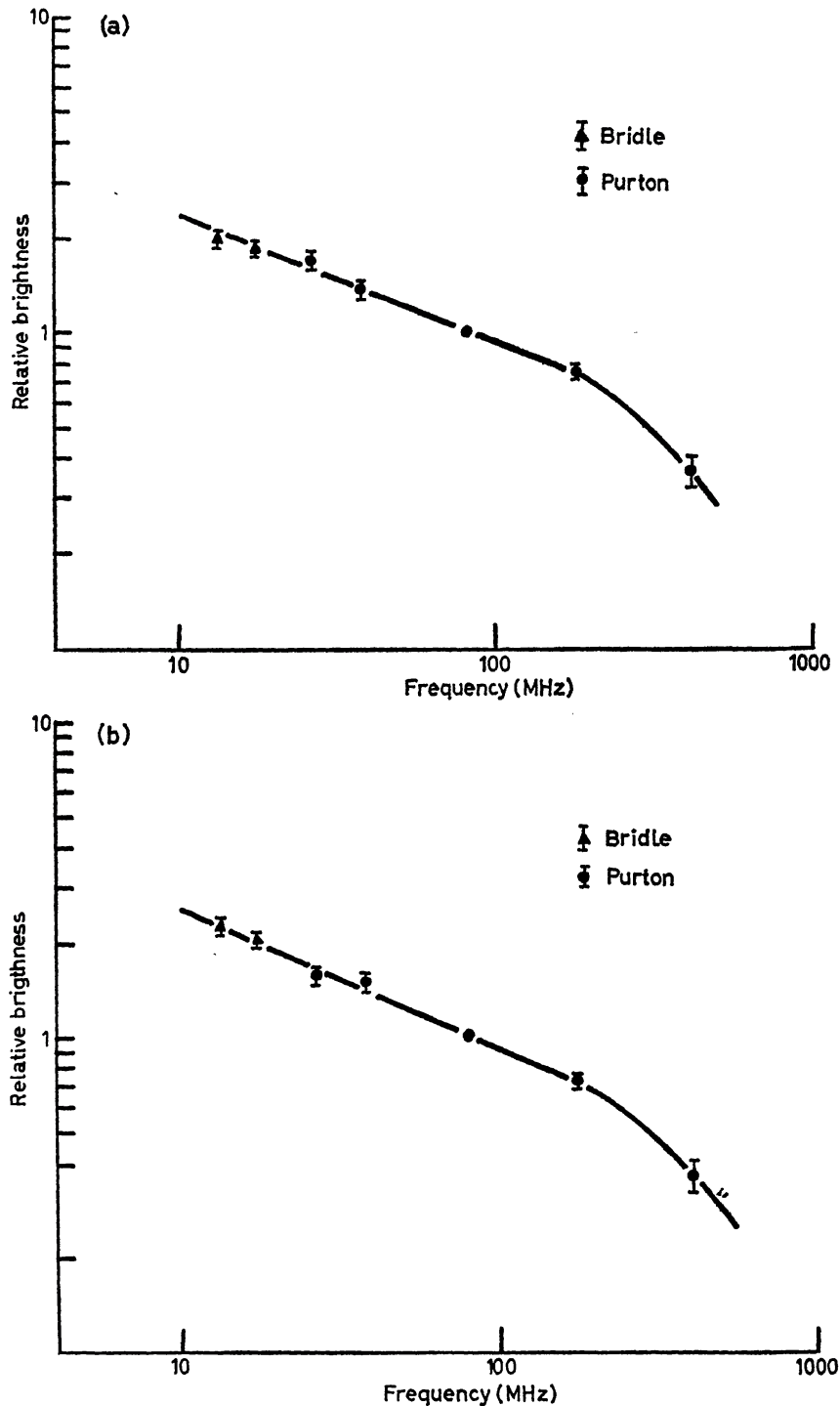

FIG. 8. *Differential spectra of Regions 1 and 2*, 13·15 *to* 404 *MHz*.
(a) *Region* 1   (b) *Region* 2

the relation $\gamma = 2\beta - 3$ from the theory of synchrotron emission (27). The value o
γ at the lower end of the energy range was apparent from the early work of Costai
(1) and was for some years regarded as a stumbling-block for the theory of th
origin of the emission (28). The difficulty arose through the assumption that th

galactic electrons are the products of high-energy proton–proton collisions; it was shown by several authors that the value of γ to be expected from this process is in the range $2 \cdot 4$–$2 \cdot 6$ at these energies (29, 30). Recent direct investigations of primary cosmic-ray electrons near the top of the Earth's atmosphere (31, 32, 33) have been carried out with sufficient accuracy to demonstrate conclusively that the actual electron energy spectrum is in good agreement with the radio data. In Fig. 9 the cosmic-ray data is shown with the energy spectrum expected from the present
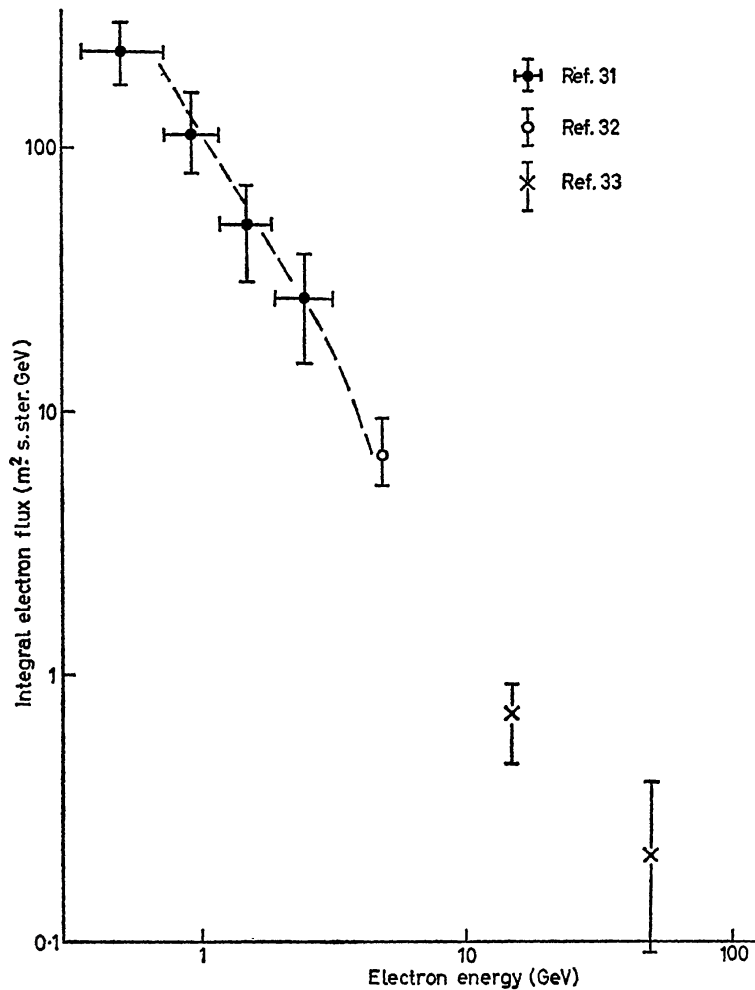
FIG. 9. *Comparison of cosmic-ray and radio data on electron energy spectrum.*

results superimposed upon it, for the assumed magnetic field $H = 5 \times 10^{-6}$ gauss. It now seems inescapable that the electrons in the energy range 750 MeV–3 GeV are not the secondary decay products of proton–proton collisions.

The interpretation of the steepening of the energy spectrum near 3 GeV implied by the radio data raises difficulties. The effects of various energy loss mechanisms on a production spectrum having a constant value of γ over the whole energy range have been summarized by Turtle (34). It is clear that a change of slope $\Delta\gamma \approx 1$ is extremely hard to explain in terms of a transition from one loss regime to another at an energy of 3 GeV. It seems necessary to consider the possibility that the change in slope indicates a change in the dominant electron production mechanism rathe than one in the dominant energy loss mechanism. This view receives support from

observations of the charge ratio of the electrons in the lower and higher parts of the energy range. Hartman, Meyer & Hildebrand (35) have shown that there is an excess of negative electrons in the energy range 100 MeV–3 GeV, whereas Daniel & Stephens (33) find an overwhelming excess of positive electrons in the range 15–50 GeV. Jones (36) has shown that the proton–proton interaction would be expected to produce a substantial excess of positive over negative charges. A tentative interpretation of the galactic electron component would therefore be as follows: at energies above about 5 GeV, the electrons are predominantly positive charges resulting from high-energy proton–proton interactions. The energy spectrum of such electrons would be compatible with the radio data if energy loss by synchrotron radiation were important. Below 3 GeV, the electrons are predominantly negative charges produced by some other process, such as the Fermi-mode acceleration of the low-energy knock-on electrons produced by the collision of the primary cosmic-ray protons with the interstellar material (37). Finally, it is noted that the observed electron energy spectrum shows a tendency to steepen at about 3 GeV, in agreement with the prediction from the radio data. With the present data this tendency is not, however, quite significant. As more accurate determinations of the primary electron energy spectrum become available, it should be possible to combine the radio and cosmic-ray data to form an independent estimate of the mean strength $\bar{H}$ of the galactic magnetic field, by combining the frequency of the break in the radio spectrum with the energy of the break in the electron spectrum. This is a research area of some interest, considering the wide range of values currently ascribed to this field by different deductive techniques (22, 25, 26).

(d) *Total spectrum of the north galactic pole.* The revised brightness temperatures of Turtle *et al.* and the lower-resolution results of the present work at 17·5 and 13·15 MHz have been used to derive brightnesses for the north galactic pole between 404 and 13·15 MHz by averaging over the four beam positions nearest to the pole in the surveys concerned. The total spectrum of the pole derived in this way is plotted on an absolute scale in Fig. 10, which also shows the results for this part of the sky of satellite-borne experiments at 3·0 and 2·3 MHz (38, 39). The spectrum obtained is straight, with $\beta = 2·55 \pm 0·04$. Wielebinski & Yates (40) have given a spectrum for the south galactic pole based on single-dipole observations at 20, 30 and 85 MHz, and this spectrum agrees well with the brightness given by Hartz (39) for that direction. Their spectrum has a value of β of $2·65 \pm 0·15$. Yates & Wielebinski (41) have measured the brightness of this region at 14·1 MHz and find a mean spectral index at 16 MHz of $2·55 \pm 0·15$. The measurements of the total spectra of the north and south galactic poles are therefore in agreement within the experimental errors.

8. *Conclusions.* It is found that even the observations of high galactic latitudes cannot be explained on a model of the emission in which the galactic contribution to the background has the same spectrum everywhere. Differential spectra with $\beta = 2·38 \pm 0·02$ and $2·45 \pm 0·03$ apply between 13·15 and 178 MHz in regions in the direction of the local spiral arm near the anticentre and in the inter-arm region respectively. There is evidence that absorption of the radiation takes place at low galactic latitudes near the anticentre at the lower frequencies, and that the

North Galactic Spur has a lower spectral index than its surroundings. The differential spectrum found for the emission from the spiral arm is compatible with observations of the energy spectrum of primary cosmic-ray electrons.
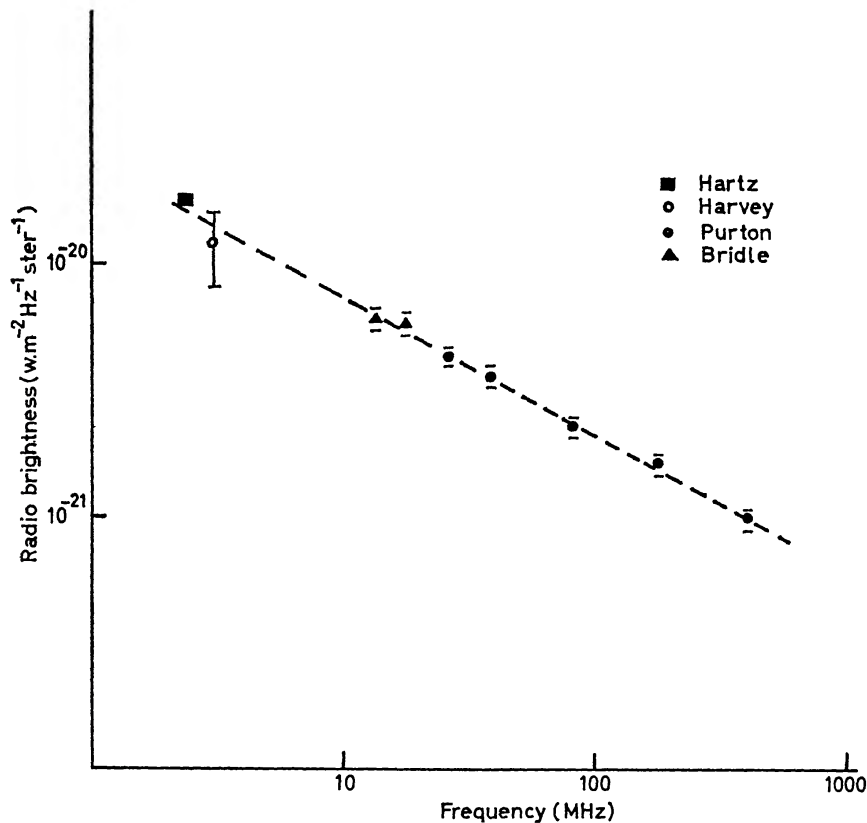

FIG. 10. *The total spectrum of the north galactic pole.*

9. *Acknowledgments.* I should like to thank Mr T. F. Howell for valuable assistance with the construction of the $13 \cdot 15$ MHz aerial, and Mr C. R. Purton for giving access to his results before publication. I am grateful to Dr J. E. Baldwin and Dr C. H. Costain for their interest in this work and for their comments on the original manuscript of this paper.

This work was performed during the tenure of an S.R.C. award, and of a research scholarship at Trinity College, Cambridge.

Mullard Radio Astronomy Observatory,
    Cavendish Laboratory,
        Cambridge.
1966 *October.*

References

(1) Costain, C. H., 1960. *Mon. Not. R. astr. Soc.*, **120**, 248.
(2) Turtle, A. J., Pugh, J. F., Kenderdine, S. & Pauliny-Toth, I. I. K., 1962. *Mon. Not. R. astr. Soc.*, **124**, 297.
(3) Purton, C. R., 1966. *Mon. Not. R. astr. Soc.*, **133**, 463.
(4) Andrew, B. H., 1966. *Mon. Not. R. astr. Soc.*, **132**, 79.
(5) Pugh, J. F., 1964. Ph.D. thesis, Cambridge University.
(6) Smith, F. G., 1961. *Proc. Instn elect. Engrs*, **108B**, 201.
(7) Mott, N. F., unpublished. Quoted by Smith, R. A., 1946. *Aerials for Metre and Decimetre Wavelengths.* Cambridge University Press.

(8) Wilson, A. C. & Cottony, H. V., 1966. N.B.S. Report No. 6017.

(9) Ellis, G. R. A., 1964. *Nature, Lond.*, **204**, 272.

(10) Oort, J. H., Kerr, F. T. & Westerhout, G., 1958. *Mon. Not. R. astr. Soc.*, **118**, 379.

(11) Hornby, J. M., 1965. Ph.D. thesis, Cambridge University.

(12) Ryle, M. & Neville, A. C., 1962, *Mon. Not. R. astr. Soc.*, **124**, 147.

(13) Williams, P. J. S. & Stewart, P., 1966. *Mon. Not. R. astr. Soc.*, in press.

(14) Erickson, W. C. & Cronyn, W. N., 1965. *Astrophys. J.*, **142**, 1156.

(15) Galt, J. A. & Costain, C. H., 1965. *Trans. R. Soc. Canada*, **3**, 419.

(16) Galt, J. A., Purton, C. R. & Scheuer, P. A. G., 1967. To be submitted to *Trans. Antennas Propag.*

(17) Longair, M. S. & Scott, P. F., 1965. *Mon. Not. R. astr. Soc.*, **130**, 379.

(18) Gower, J. F. R., 1966. *Mon. Not. R. astr. Soc.*, **133**, 151.

(19) Turtle, A. J. & Baldwin, J. E., 1962. *Mon. Not. R. astr. Soc.*, **124**, 459.

(20) Longair, M. S., 1966. *Mon. Not. R. astr. Soc.*, **133**, 421.

(21) Shain, C. A., 1958. I.A.U./U.R.S.I. *Symposium on Radio Astronomy*, Paris, p. 328. Stanford University Press.

(22) Wentzel, D., 1963. *A. Rev. Astr. Astrophys.*, **1**, 195.

(23) Earl, J. A., 1961. *Phys. Rev. Lett.*, **6**, 125.

(24) Parker, E. N., 1965. *Planet Space Sci.*, **13**, 9.

(25) Morris, D., Clark, B. G. & Wilson, R. W., 1963. *Astrophys. J.*, **138**, 889.

(26) Weinreb, S., 1962. *Astrophys. J.*, **136**, 1149.

(27) LeRoux, E., 1961. *Annls Astrophys.*, **24**, 71.

(28) Smith, F. G., 1961. *Nature, Lond.*, **191**, 1381.

(29) Hayakawa, S. & Okuda, H., 1962. *Prog. theor. Phys.*, **28**, 517.

(30) Ginzburg, V. I. & Syrovatskii, S. I., 1964. *The Origin of Cosmic Rays*. Pergamon Press.

(31) L'Heureux, J. & Meyer, P., 1965. *Phys. Rev. Lett.*, **15**, 93.

(32) Agrinier, B., Koechlin, Y., Parlier, B., Boella, G., Degli Antoni, G., Dilworth, C., Scarsi, L. & Sironi, G., 1964. *Phys. Rev. Lett.*, **13**, 377.

(33) Daniel, R. R. & Stephens, S. A., 1965. *Phys. Rev. Lett.*, **15**, 769.

(34) Turtle, A. J., 1963. *Mon. Not. R. astr. Soc.*, **126**, 405.

(35) Hartman, R. C., Meyer, P. & Hildebrand, R. H., 1965. *J. geophys. Res.*, **70**, 2713.

(36) Jones, F. C., 1965. *Phys. Rev. Lett.*, **15**, 512.

(37) Brunstein, K. A., 1965. *Phys. Rev.*, **137B**, 757.

(38) Harvey, C. C., personal communication.

(39) Hartz, T. R., 1964. *Nature, Lond.*, **203**, 173.

(40) Wielebinski, R. & Yates, K. W., 1965. *Nature, Lond.*, **205**, 581.

(41) Yates, K. W. & Wielebinski, R., 1965. *Nature, Lond.*, **208**, 64.